

Cortico-brainstem mechanisms of biased perceptual decision-making in the context of pain

Running title: **Neural basis of perceptual bias in pain**

Katja Wiech^{1*}, Falk Eippert^{1,2*}, Joachim Vandekerckhove^{3,4}, Jonas Zaman⁵, Katerina
Placek⁶, Francis Tuerlinckx⁴, Johan Vlaeyen^{5,7}, Irene Tracey¹

* These authors contributed equally

- ¹ Wellcome Centre for Integrative Neuroimaging (WIN), Nuffield Department of Clinical Neurosciences, University of Oxford, John Radcliffe Hospital, Headley Way, Oxford OX3 9DU, UK
- ² Max Planck Institute for Human Cognitive and Brain Sciences, Stephanstrasse 1a, 04103 Leipzig, Germany
- ³ Department of Cognitive Sciences, 2201 Social & Behavioral Sciences, Gateway Building (SBSG), University of California, Irvine, CA 92697-5100, USA
- ⁴ Research Group of Quantitative Psychology and Individual Differences, KU Leuven, Tiensestraat 102, 3000 Leuven, Belgium
- ⁵ Research Group Health Psychology, KU Leuven, Tiensestraat 102, 3000 Leuven, Belgium
- ⁶ Takeda Pharmaceuticals, Statistics and Quantitative Sciences, Cambridge MA, USA
- ⁷ Research Group Experimental Health Psychology, Maastricht University, 6200 Maastricht, Netherlands

Corresponding author:

Katja Wiech, PhD
Nuffield Dept. of Clinical Neurosciences (Nuffield Division Anaesthetics) & Wellcome
Centre for Integrative Neuroimaging (WIN Centre)
John Radcliffe Hospital, University of Oxford, Oxford, OX3 9DU
phone: +44 1865 222545 | fax: +44 1865 222717 | email: katja.wiech@ndcn.ox.ac.uk

Number of pages: 42
Number of figures: 6

Disclosures

K.W. has received Consultancy fees from P&G Health, Germany. I.T. is on the Neuroscience Scientific Advisory Board of Amgen, the Council of Medical Research Council and the Grete Lundbeck Brain Prize Committee. She is also a Trustee of BRAIN and MQ Mental Health Charity and part of Innovative Medicines Initiative PainCare-Biopain. K.P. is a full-time employee of Takeda Pharma; the present publication has

been prepared independently and outside of the employment; the employer is not involved in any of the subjects dealt within this publication and did not provide any form of support. All other authors have no conflict of interest to declare.

K.W. was supported by an MRC UK New Investigator grant (MR/L011719/1). F.E. is supported by the Max Planck Society and the European Research Council (ERC StG 758974). J. Zaman is a postdoctoral research fellow of the Research Foundation Flanders (FWO, 12P8619N) and was supported by the EFIC-Grünenthal grant. J.W.S.V. was supported by the Odysseus grant “The Psychology of Pain and Disability Research Program” funded by the Research Foundation Flanders, Belgium (FWO Vlaanderen, Belgium), and is supported by the “Asthenes” long-term structural funding Methusalem grant by the Flemish Government, Belgium (METH/15/011). F.T. was supported by KU Leuven Research Council Grant GOA/15/003 and the Fund for Scientific Research–Flanders (Grants G.0534.09N and G.0806.13). J.V. was supported by the Belgian National Science Foundation grant #1658303. I.T. was supported by the Wellcome Trust (090955/Z/09/Z and 083259/Z/07/Z) and Medical Research Council, UK (G0700399).

The Wellcome Centre for Integrative Neuroimaging is supported by core funding from the Wellcome Trust (203139/Z/16/Z).

Abstract

Prior expectations can bias how we perceive pain. Using a drift diffusion model, we recently showed that this influence is primarily based on changes in perceptual decision-making (indexed as shift in starting point). Only during unexpected application of high-intensity noxious stimuli, altered information processing (indexed as increase in drift rate) explained the expectancy effect on pain processing. Here, we employed functional magnetic resonance imaging to investigate the neural basis of both these processes in healthy volunteers. On each trial, visual cues induced the expectation of high- or low-intensity noxious stimulation or signalled equal probability for both intensities. Participants categorised a subsequently applied electrical stimulus as either low- or high-intensity pain. Shift in starting point towards high pain correlated negatively with right dorsolateral prefrontal cortex (rDLPFC) activity during cue presentation underscoring its proposed role of “keeping pain out of mind”. This anticipatory rDLPFC signal increase was positively correlated with periaqueductal gray (PAG) activity when the expected high-intensity stimulation was applied. Drift rate increase during unexpected high-intensity pain was reflected in amygdala engagement and increased functional connectivity between amygdala and PAG. Our findings suggest involvement of the PAG in both decision-making bias and altered information processing to implement expectancy effects on pain.

Perspective

Modulation of pain through expectations has been linked to changes in perceptual decision-making and altered processing of afferent information. Our results suggest involvement of the dorsolateral prefrontal cortex, amygdala, and periaqueductal gray in these processes.

Keywords: perceptual decision-making, amygdala, bias, prefrontal, expectation, periaqueductal gray

Introduction

Expectations critically shape the way we perceive pain: the same noxious input is, for instance, experienced as significantly more intense when we expect it to be of a high intensity.^{3,8,33,49,70} Such effects are often thought to be accompanied by changes in somatosensory processing. Using a perceptual decision-making task in combination with a model-based approach employing a Hierarchical Drift Diffusion model^{53,63}, we recently investigated whether the influence of expectations on pain perception could also be rooted in biased perceptual decision-making.⁶⁷ Faster processing of incoming sensory information (indexed by the model parameters ‘drift rate’) indicates an effect on sensory processing. In contrast, biased decision-making (indexed by a shift in the model parameter ‘starting point’) indicates that less evidence is needed to categorise a sensation as suggested by prior information (e.g., as high-intensity pain when high-intensity pain is expected) compared to a neutral starting point. A direct comparison of both hypotheses confirmed the dominant influence of biased decision-making: cues signaling a higher probability of either low-intensity or high-intensity stimulation introduced a decision bias towards the expected stimulation intensity rather than a change in sensory processing.

Brain imaging studies have begun to unravel the neural underpinnings of such biased perceptual decision-making^{15,30,43,48}, with evidence linking activity in the dorsolateral prefrontal cortex (DLPFC) to a shift in starting point.⁴² However, these findings originate from studies using affectively neutral stimuli (e.g., moving dots) and might not be applicable to the affect-rich domain of pain, giving rise to two possible scenarios. If DLPFC activity reflects the degree to which a perceptual decision is biased,

cue-induced activity should be positively related to a shift in starting point towards the expected sensation, irrespective of the affective value, i.e. whether low or high pain is expected. If these responses are instead sensitive to the affective value of a choice, cue-induced activity could show a different, affect-dependent relation with a shift in starting point. Based on previous neuroimaging studies on pain which have specifically implicated DLPFC regions in the expectation of reduced pain², one would expect a positive correlation with decision bias if low pain is expected and a negative correlation with decision bias when high pain is expected. Such finding would call into question the domain-generalty of the above-mentioned pattern of DLPFC responses, but would sit nicely with the known DLPFC involvement – together with the rostral anterior cingulate cortex (rACC) and the periaqueductal grey (PAG) – in descending pain control.^{2,58,62}

We also explored altered somatosensory processing (indexed as change in drift rate), which we had previously observed in the ‘worst-case’ scenario of high-intensity noxious stimuli being unexpectedly received.⁶⁷ In line with the assumption of altered somatosensory processing during expectancy-induced pain modulation, a change in drift rate should lead to activation changes in brain regions linked to somatosensory processing as well as the amygdala, which adjusts the sensitivity of sensory cortices depending on the perceived threat of the incoming sensory information.^{21,28,51,55}

Here we explored the neural processes underlying both biased decision-making and altered somatosensory processing in the context of pain using functional magnetic resonance imaging (fMRI) in healthy volunteers. Model parameters were calculated based on response times and decision accuracies obtained during a perceptual decision-making task in which participants had to indicate whether a high or low-

intensity stimulus had been applied following the presentation of a visual cue that signaled the probability of both intensities.

Methods

The experimental paradigm and procedures as well as the analysis of the behavioural data including computational modeling have been described in detail in a previous publication.⁶⁷ An overview of the paradigm is provided in Fig. 1. The data presented here are based on these findings but focus on the fMRI data acquired in the same experiment.

Participants. Twenty-two healthy volunteers (11 female; age $M = 25.95$ years, $SD = 4.20$) participated in the study. Sample size estimation was based on a previous study¹ investigating expectancy effects on pain using fMRI ($N = 19$) and studies with a sample size of $N = 20$ ⁴³ and $N = 24$ ⁶⁶ exploring expectancy effects on perceptual decisions using a drift diffusion model in combination with fMRI .

Participants were right-handed, fluent English-speaking, displayed normal pain thresholds at the site of stimulus application, and had normal or corrected-to-normal vision. According to self-report, no participant had a history of neurological or psychiatric disease or of chronic pain. Prior to involvement in the study, each participant gave full informed consent, and the study was approved by the local Research Ethics Committee (MSD-IDREC-C1-2013-106).

Experimental paradigm. Using fMRI, we investigated brain responses during the anticipation and perception of high and low-intensity noxious electrical stimuli. The experiment was divided into four blocks, each consisting of 42 trials. On each trial, participants were presented with one of three visual cues (see Fig. 1): the white outline of a square, a triangle or a circle against a black background. One of these three cues indicated an 80% probability for high-intensity stimulation and a 20% probability for low intensity stimulation ('80/20' condition; note that the first number always refers to the probability of a high intensity stimulation, the second one to the probability of a low intensity stimulation). Another cue indicated a 20% probability for high-intensity stimulation and an 80% probability for low intensity stimulation ('20/80' condition). A third cue indicated a 50% probability for high-intensity stimulation and a 50% probability for low intensity stimulation ('50/50' condition). The three visual cues were randomly assigned to the 80/20, 20/80, and 50/50 conditions across participants, resulting in six different configurations of cue and condition pairings. In each configuration, the order of trials (e.g., first trial: 80/20 condition, second trial: 50/50 condition, third trial: 20/80 condition, fourth trial: 50/50 condition etc.) was the same in each of the four blocks.

- insert Figure 1 about here -

On each trial, either a high-intensity or a low-intensity stimulus was applied to the dorsal aspect of the left hand five seconds after presentation of the visual cue. Participants were instructed to indicate as quickly and accurately as possible whether they had received low-intensity or high-intensity stimulation by pressing one of two

buttons with their right hand. Button-response contingencies were counter-balanced across participants. No feedback was provided regarding the correctness of the response on any trial. Decision accuracies and response times (RT; i.e. time between delivery of noxious stimulus and button pressing) were recorded. Each trial was completed by the presentation of a fixation cross for three, five, or seven seconds. The order of 80/20, 20/80, and 50/50 trials was pseudo-randomized with no more than two consecutive trials of the same type.

In preparation for the experiment, participants were first familiarized with the visual and electrical stimuli and instructed about the pairing between the three visual cues and the outcome probabilities before they practiced providing their responses outside the MR scanner. Next, individual high and low-intensity stimulation levels were determined using a standardized calibration procedure²⁴. To test whether differential learning had been instantiated, participants underwent a discrimination test before they completed a practice run of the actual experiment and were subsequently positioned in the scanner. In this stimulation discrimination test, ten low-intensity stimuli and ten high-intensity stimuli were applied in a randomized order. Participants had to verbally categorize each stimulus as either a low-intensity or a high-intensity stimulus. Only participants who were able to categorise at least 80% of trials correctly were admitted to the actual experiment. Those with categorization accuracies <80% underwent re-calibration of the stimulus intensities and completed a second practice run. None of the participants had to be excluded based on these criteria. In addition, participants completed a short test that probed their understanding of cue-stimulation contingencies. Each cue was presented ten times in a randomized order and participants had to verbally indicate whether the cue signaled a high-intensity

stimulation in 80%, 50% or 20% of trials. Note that participants were explicitly informed about the contingencies prior to the performance test. If participants were able to categorize at least 80% of the trials correctly, they were positioned in the MR scanner and the experiment commenced. All participants demonstrated sufficient contingency awareness at the first practice run.

Electrocutaneous stimulation. Individual levels for high and low-intensity stimulation were determined for each participant using an ascending Method of Limits approach.²⁴ Intensities were rated on a Visual Analogue Scale (VAS) with the verbal anchor point “no pain” for the minimum intensity and “unbearable pain” for the maximum intensity. Participants were instructed that only if the cursor was positioned at the very left of the scale (marked as “no pain”) would the sensation be recorded as non-painful. VAS ratings were transformed into a number between 0 and 10. Intensities rated as 2 were used for low-intensity pain, and intensities rated as 8 were used for high-intensity pain. Electrical stimuli were delivered using a commercial electric stimulation device (constant current stimulator DS7A; Digitimer, Hertfordshire, UK), delivering a 1ms monopolar square waveform pulse via a concentric silver chloride electrode attached to the back of the left hand. The average stimulation intensity across participants was 2.01 mA ($SD= 1.54$) for low-intensity stimuli and 8.20 mA ($SD= 4.15$) for high-intensity stimuli. The two stimulation intensities were rated as significantly different ($t(21)= 5.02$; $p< 0.001$). The calibration procedure was first performed during preparation outside the scanner and both stimulation intensities were checked again and recalibrated if necessary, once

participants were positioned in the scanner and prior to each block to ensure constant pain levels throughout the experiment.

fMRI data acquisition. Functional imaging was performed on a 3-Tesla MRI scanner (Siemens Verio, Siemens Medical Solutions) equipped with a 32-channel head coil. T2*-weighted echo-planar volumes with BOLD contrast were acquired at an angle of 30° to the anterior commissure-posterior commissure line to attenuate signal dropout in the orbitofrontal cortex¹² using a multiband EPI sequence (slice acceleration factor: 6^{41,69}). A total of seventy-two transverse slices were acquired with an interleaved order for each volume, with an isotropic in-plane resolution of 2 mm and slice thickness of 2 mm (repetition time, TR: 1300 ms; echo time, TE: 40 ms; field of view, FoV: 212 x 212 mm²; flip angle: 66°). A whole-brain high-resolution T1-weighted MP-RAGE structural scan (interpolated voxel size: 1x1x1 mm³; TR: 2040 ms; TE: 4.7ms; FOV: 192 x 174mm²; 192 partitions; flip angle: 8 degrees; inversion time, TI: 900 ms) was also obtained for each participant.

fMRI data analysis: general aspects. Image processing and statistical analyses were performed using SPM12 (Wellcome Department of Imaging Neuroscience, London, UK; available at <http://www.fil.ion.ucl.ac.uk/spm>). Image processing consisted of slice timing (correction for differences in slice acquisition time), realignment (rigid body motion correction) and unwarping (accounting for susceptibility by movement interactions), coregistration (between EPI images and the skull-stripped T1 image), spatial normalization using the DARTEL toolbox, smoothing using an 8mm (full width at half maximum) isotropic three-dimensional Gaussian kernel and denoising using ICA-AROMA.⁵²

For each participant, we constructed a design matrix that included three regressors for the anticipation phase (presentation of (i) the 50/50 cue, (ii) the 80/20 cue, and (iii) the 20/80 cue) and six regressors for the stimulus delivery phase (delivery of the low-intensity stimulation following (i) the 50/50 cue, (ii) the 80/20 cue, and (iii) the 20/80 cue and delivery of the high-intensity stimulation following (iv) the 50/50 cue, (v) the 80/20 cue, and (vi) the 20/80 cue), resulting in a total of nine regressors. All regressors consisted of delta functions convolved with the canonical hemodynamic response function. Six motion parameters derived from the realignment procedure were also included as regressors-of-no-interest. Model estimation was carried out using a robust weighted least squares approach¹⁴ and also included high-pass filtering (cutoff period: 128 s) and correction for temporal autocorrelations (based on a first-order autoregressive model).

Based on the first-level model, we defined contrasts of parameter estimates for each participant (see below) and subsequently explored the relation between individual modeling parameters (as derived using a Hierarchical Drift Diffusion model, HDDM⁶³) and individual brain responses by means of regression analyses at the group level (for main effects during anticipation and stimulation period see <https://osf.io/2k8yf/>). A HDDM is suitable for perceptual decision-making tasks in which participants are required to choose between two response options on each trial (i.e., high and low pain) and has previously been applied in studies using visual²³, auditory⁶⁰, non-noxious and noxious somatosensory stimuli.^{71,72} Modeling parameters considered here include the shift in starting point (indicating biased perceptual decision-making) and the change in drift rate (indicating altered sensory processing), always compared to the neutral 50/50 condition. Both parameters had been estimated for each participant

as described in our previous publication⁶⁷ for individual parameter estimates see <https://osf.io/2k8yf/>). In brief, we fitted the HDDM with four parameters (starting point, β ; drift rate, δ ; boundary separation, α ; and non-decision time τ) using correct and incorrect trials. Drift rate and non-decision time parameters were allowed to differ between the six outcome conditions of the experiment (i.e., low-intensity stimulation following the '80/20' cue, the '20/80' cue or the '50/50' cue and high-intensity stimulation following the '80/20' cue, the '20/80' cue or the '50/50' cue). Boundary separation and starting point were only allowed to differ as a function of task instruction ('80/20' during anticipation, '20/80' during anticipation or '50/50' during anticipation) because both parameters are determined prior to stimulus delivery. Note that the precision with which posterior distributions are estimated under the Bayesian framework (detailed in our previous publication⁶⁷) accounts for differences in the number of trials (e.g., lower number of error trials than correctly classified trials).

The regression analyses presented below are based on the significant behavioral effects reported in our previous publication⁶⁷, which included a shift in starting point towards high pain when high pain is expected, a shift in starting point towards low pain when low pain is expected and an increase in drift rate when the high-intensity stimulation was unexpectedly applied (boundary separation and non-decision time were not investigated here, due to non-significant effects in our previous study). In all analyses, HDDM model parameters for the relevant condition were compared to those of the '50/50' condition in which both outcomes were equally likely. These subject-specific differential model parameters were entered into simple regression

analyses at the group level. In keeping with the differential HDDM modeling parameters, differential contrast images comparing the condition of interest with the non-informative '50/50' condition were used as specified below. These analyses (as well as follow-up analyses on significant findings) are explained in detail below.

In all of our fMRI analyses, statistical inference was based on voxel-wise non-parametric permutation testing⁶⁸ as implemented in SnPM (Statistical nonparametric Mapping; version SnPM 13.1.02; <http://niso.org/Software/SnPM13/>) using a threshold of $p < 0.05$ with family-wise error correction for both hypothesis-free whole-brain analyses and hypothesis-driven region-of-interest (ROI) analyses. ROIs for the current study included brain areas that are often ascribed a 'pain modulatory' role (DLPFC, rACC, amygdala, and PAG), as well as somatosensory brain areas that typically respond to noxious stimulation (thalamus, primary and secondary somatosensory cortex (SI, SII), posterior insula). Masks of these ROIs were derived from probabilistic atlases included with FSL (FMRIB's Software Library; <https://fsl.fmrib.ox.ac.uk/fsl/fslwiki/Atlases>), all thresholded at 25%. In the case of cortical ROIs these masks were intersected with the participants' average gray matter mask in order to exclude white matter regions of no interest. SI, SII, and posterior insula were based on the Jülich Histological Atlas¹⁸ (SI (mask is a union of areas 1, 2, 3a, 3b)^{25–27}; SII (mask is a union of areas OP1, OP2, OP3, OP4)^{16,17}; posterior insula (mask is a union of areas lg1, lg2, ld1)³⁶, the thalamus mask was based on the Thalamic Connectivity Atlas⁵ (mask is a union of all areas), the amygdala mask was based on the Harvard-Oxford Atlas¹³, the PAG mask was based on the PAG Atlas²⁰; mask is a union of all areas), the DLPFC was based on the Dorsal Frontal Connectivity Atlas⁵⁷; mask is a union of areas 9/46d and 9/46v) and the rACC was based on the Cingulate

Orbitofrontal Connectivity Atlas⁴⁵; mask is a union of areas 32d and 32pl). Note that we provide unthresholded whole-brain maps of uncorrected p-values (again based on non-parametric permutation testing) for each tested effect at <https://neurovault.org/collections/SHQGGEGD> in order to aid interactive exploration of our data and to facilitate meta-analytic efforts. Furthermore, we provide effect size estimations for all key findings (see <https://osf.io/2k8yf/>) following recent recommendations.⁵⁰

fMRI data analysis: anticipatory activity related to shift in starting point. In order to test whether the DLPFC would show activation related to the degree to which the starting point had been shifted towards the high pain boundary, we performed a regression analysis on the differential imaging contrast between the presentation of the high pain cue and the non-informative cue ('80/20 cue' minus '50/50 cue') and used the relative shift in starting point between both conditions ('80/20' minus '50/50') as the regressor-of-interest.

In order to test whether activation in the DLPFC also scaled with a shift in starting point towards low-intensity pain, we regressed the modeling parameters for the condition in which participants were cued towards low-intensity stimulation ('20/80' condition relative to the non-informative '50/50' condition) against the equivalent imaging contrast (i.e., '20/80 cue' minus '50/50 cue'). Note that as starting point scores can vary between 0 (strongest possible bias towards low pain) and 1 (strongest possible bias towards high pain), the difference score between (numerically smaller) starting point indicating a bias towards low pain and a (numerically higher) starting point indicating no bias (as in the '50/50' condition) would be negative. We therefore

use the absolute value of the difference in starting point between both conditions (i.e., |‘20/80 cue’ minus ‘50/50 cue’|) which provided positive difference scores in all participants as starting point scores were higher for the ‘50/50’ than the ‘20/80’ condition in all cases. Although our hypotheses meant we focused analyses on the DLPFC (where we applied small-volume corrections separately for the right and left hemisphere), whole-brain analyses were additionally carried out, but revealed no significant results at a level of $p < 0.05$ FWE.

fMRI data analysis: effects of anticipatory DLPFC activity. As explained in more detail in the results section, the previous analyses revealed a *negative* correlation between activation in DLPFC during cue presentation and the degree to which participants had shifted the starting point towards high pain. In order to investigate how this DLPFC engagement during the *cue period* translated into the *stimulation period* (i.e. when noxious stimuli were delivered), we performed two follow-up analyses. Individual parameter estimates were extracted from the identified DLPFC peak using the same contrast (i.e., ‘80/20 cue’ minus ‘50/50 cue’). These parameter estimates were entered as a regressor-of-interest in a group level regression analysis using the differential imaging contrast (‘80/20’ minus ‘50/50’) modeling activation during *stimulus delivery* (i.e., after the anticipation phase). Because the high pain cue could either be followed by low or high intensity stimulation, both trial types were analyzed separately: one analysis focused on trials in which high-intensity stimulation was delivered following the 80/20 cue (i.e., ‘80/20 cue followed by high-intensity stimulation’ minus ‘50/50 cue followed by high-intensity stimulation’) and another analysis focused on trials in which low-intensity stimulation was delivered (i.e., ‘80/20

cue followed by low-intensity stimulation' minus '50/50 cue followed by low-intensity stimulation').

The previous finding of a *positive* correlation between DLPFC activation and a shift in starting point towards low pain when low-intensity stimulation was the more likely outcome ('50/50 cue' minus '20/80 cue'; see Results for details) was followed up in a similar way: individual parameter estimates were extracted from the DLPFC peak identified in this analysis and entered as a regressor-of-interest into the imaging analysis testing for activity either during the unexpected delivery of high-intensity stimulation ('20/80 cue followed by high-intensity stimulation' minus '50/50 cue followed by high-intensity stimulation') or during the expected delivery of low-intensity stimulation ('20/80 cue followed by low-intensity stimulation' minus '50/50 cue followed by low-intensity stimulation').

Based on the tight link between DLPFC, rACC and PAG in descending pain modulation^{7,19,59,65}, we applied small-volume correction to the rACC and PAG in these analyses (whole-brain analyses were also carried out but revealed no significant results at a level of $p < 0.05$ FWE).

fMRI data analysis: stimulation period activity related to an increase in drift rate. As reported in our previous publication⁶⁷, the unexpected application of a high-intensity electrical stimulus led to an increase in drift rate. To test our hypothesis of whether brain regions involved in pain-related sensory processing and the amygdala reflected this change in somatosensory processing, we performed a regression analysis using the difference between the drift rate of the condition in which participants had been cued towards low pain, but received a high-intensity stimulus ('20/80' condition with

high-intensity stimulation) and the neutral '50/50' condition with high-intensity stimulation as a regressor-of-interest for the differential contrast image of both conditions (i.e., '20/80' condition with high-intensity stimulation minus '50/50' condition with high-intensity stimulation). Given our hypotheses, these analyses focused on somatosensory regions (thalamus, SI, SII and posterior insula) as well as the amygdala, where we applied small-volume corrections (whole-brain analyses were also carried out and revealed one significant response in the left hippocampus: $x,y,z = -30,-14,-10$; $t = 6.49$; $p = 0.035$ FWE).

fMRI data analysis: connectivity changes related to an increase in drift rate. In order to investigate the functional connectivity of the drift rate related amygdala activation identified in the previous analysis we conducted a psychophysiological interaction analysis²² using the left and right amygdala peaks as seed regions in two separate analyses. For each individual we first extracted the BOLD time-series from the peak voxel of the left and right amygdala activation identified in ($x,y,z = -26,-8,-14$ for left amygdala and $x,y,z = 26,-2,-12$ for right amygdala). Next, a PPI regressor was computed as the element-by-element product of the mean-corrected amygdala activity and a vector coding for the condition in which a high-intensity stimulus was unexpectedly applied compared to high-intensity stimulation following the non-informative cue (i.e. '20/80' high pain minus '50/50' high pain). The first-level PPI model included the PPI regressor as well as the activation time course in the amygdala and the psychological variable (i.e., the difference between '20/80' high pain and '50/50' high pain) as regressors-of-no-interest. The individual contrast images reflecting the interaction were subsequently entered into a second-level regression analysis with the individual

difference in drift rate between both conditions (i.e., '20/80' high-intensity stimulation minus '50/50' high-intensity stimulation) as the regressor-of-interest. While our initial hypothesis was that the unexpected delivery of a high-intensity stimulation should alter the information exchange between amygdala and brain regions related to somatosensory processing (SI, SII, thalamus and posterior insula), we also explored the possibility that such a scenario could lead to enhanced connectivity between the amygdala and the PAG, as suggested by a large line of evidence from the fear conditioning literature.^{32,39,46,61} We thus carried out small volume corrections for these regions, but also ran whole-brain analyses, which however revealed no significant results at a level of $p < 0.05$ FWE.

Results

Based on the computational modeling of decision accuracies and response times using a hierarchical drift diffusion model as described in our previous publication,⁶⁷ our interrogation of the fMRI data focused on three reported behavioural effects: the shift in starting point towards high pain during the expectation of high-intensity stimulation, the shift in starting point towards low pain during the expectation of low-intensity stimulation, the increase in drift rate when a low-intensity stimulation was expected but a high-intensity stimulus was unexpectedly delivered (Fig. 2), and follow up analyses based on results from these.

- insert Figure 2 about here -

Anticipatory activity related to shift in starting point. Analyses investigating the shift in starting point towards high pain did not provide evidence for a positive correlation, but instead revealed a negative correlation between the relative shift in starting point towards the high pain boundary and activation in the right DLPFC ($x,y,z = 22,36,52$; $t = 4.35$; $p = 0.023$; Fig. 3A,B). In other words, the more participants activated the DLPFC during the cue period when they were expecting the high-intensity stimulation (relative to the '50/50' condition), the weaker was their decision-making bias towards high pain. When performing the same analysis for a shift in starting point towards low pain, we observed a positive correlation with right DLPFC activity ($x,y,z = 48,30,34$; $t = 4.28$; $p = 0.025$ and $x,y,z = 46,22,42$; $t = 3.98$; $p = 0.043$; Fig. 3C,D). So, the more participants activated the DLPFC during the cue period when they were expecting the low-intensity stimulation (relative to the '50/50' condition), the stronger was their decision-making bias towards low pain. A post hoc analysis investigating the spatial layout of these responses showed that 'bias towards low pain' DLPFC activity only overlapped with 'bias towards high pain' DLPFC activity at a very lenient threshold of $p < 0.05$ uncorrected. Together, these results stand in clear opposition to the pattern of DLPFC responses observed in affectively neutral decision-making scenarios, and instead suggest that they might be related to preparatory 'protective' function.

- Insert Figure 3 about here -

Effects of anticipatory DLPFC activity. In order to further explore the pain relevance of this affect-dependent anticipatory engagement of the DLPFC, we tested whether

DLPFC activation during *stimulus anticipation* (i.e., related to the shift in starting point) would predict activation in down-stream regions of the descending pain control system, namely rACC and PAG, during *stimulus application*. While we investigated both shifts in starting point (i.e., towards low pain and towards high pain) in combination with the actual delivery (i.e., delivery of high pain and delivery of low pain), we only observed a DLPFC-dependent recruitment of the descending pain control system during the expected delivery of high pain (i.e., delivery of high-intensity stimulus following presentation of the '80/20' cue). In this case, the identified DLPFC activation during *stimulus anticipation* was positively related to PAG engagement during *stimulus application* ($x,y,z = 2,-30,-10$; $t = 3.49$; $p = 0.016$ and $x,y,z = -2,-28,-10$; $t = 3.48$; $p = 0.017$; Fig. 4). Such a relationship (or its inverse) was neither observed when expectations were violated (i.e., delivery of low pain when cued about high or delivery of high pain when cued about low pain) nor when the expectation of low pain was confirmed.

- Insert Figure 4 about here -

Stimulation period activity related to an increase in drift rate. Turning to changes in sensory processing, we found a significant association between an increase in drift rate and activation in the left and right amygdala (left: $x,y,z = -26,-8,-14$; $t = 6.02$; $p = 0.002$; right: $x,y,z = 26,-2,-12$; $t = 4.16$; $p = 0.041$; Fig. 5) when expectations were violated towards the worse. In other words, the stronger the amygdala responses, the higher the increase in drift rate during the application of high-intensity stimuli that followed a cue signaling delivery of a low intensity stimuli. Contrary to our hypothesis, such a

relationship was only observed in the amygdala, but not in brain regions related to somatosensory processing (i.e., thalamus, SI, SII and posterior insula).

- Insert Figure 5 about here -

Connectivity changes related to an increase in drift rate. In order to further explore the consequences of the drift rate related amygdala responses during the ‘worst case scenario’ (i.e., delivery of high-intensity stimulation when low-intensity stimulation was more likely), we carried out psychophysiological interaction analyses seeded in the amygdala. These analyses showed a context-dependent increase in functional connectivity between the left amygdala and the PAG ($x,y,z = -2,-36,-10$; $t = 3.68$; $p = 0.010$; $x,y,z = 4,-28,-4$; $t = 3.51$; $p = 0.014$; Fig. 6), but did not provide evidence for the hypothesized increase in connectivity with somatosensory brain regions (i.e., SI, SII, thalamus and posterior insula).

- Insert Figure 6 about here -

Discussion

The present study investigated neural processes underlying pain-related perceptual decision-making. We found that activity in the DLPFC reflected a direction-specific decision-making bias (change in starting point). While a bias towards low-intensity pain was positively correlated with DLPFC activity, a bias towards high-intensity pain

showed a negative correlation with activity in the DLPFC (i.e., expectations of high-intensity pain induced less bias towards high pain judgments the more the DLPFC was engaged prior to stimulus application). This anticipatory DLPFC activity during expectation of a high-intensity stimulation was linked to increased PAG activity during stimulus receipt. Changes in sensory processing (change in drift rate) were related to heightened signal levels in the amygdala and increased functional connectivity with the PAG.

Using a similar modeling approach to the one adopted here, but employing affectively neutral stimuli, previous studies had linked a shift in starting point to increased DLPFC activity.^{43,44} Our data obtained using affectively laden noxious stimuli confirm these observations but paint a more nuanced picture. In line with previous findings, anticipatory DLPFC activity scaled positively with the shift in starting point towards low pain when participants expected low-intensity stimulation (Fig. 3). However, a *negative* relationship was found when high-intensity pain was expected (Fig. 3), albeit in a slightly different part of the DLPFC (only at an extremely liberal level of $p < 0.05$ uncorrected did we start to see an overlap between both DLPFC findings). Together, these two findings challenge the notion of a direction-insensitive DLPFC involvement in bias implementation, and suggest that its engagement depends on the nature of the expected stimulus. The DLPFC is known to be pivotal for the down-regulation of pain⁵⁸ and more specifically for initiating top-down modulation prior to stimulus encounter.³⁵ Our findings are compatible with such a role in preparing the organism for stimulus encounter which is further supported by the observation that DLPFC activity in perceptual decision-making peaks during stimulus anticipation, not during stimulus receipt.¹⁰ Our results therefore provide further evidence for a role of

anticipatory DLPFC activity in buffering against a bias towards high pain (or ‘keeping pain out of mind’³⁷) and supporting a bias towards low pain when prior information predicts low-intensity pain. Of note, DLPFC activity related to evidence accumulation has predominantly been found in the left hemisphere^{9,29} whereas our findings were localized on the right side (Fig. 3), a difference that remains to be explored. Although further studies are needed to confirm our findings, the results suggest that stimulation of the DLPFC (e.g., through non-invasive brain stimulation or neurofeedback) could be a promising target to enhance endogenous pain regulation in clinical populations.

The DLPFC is known to be embedded into a wider network of brain regions which complement its modulatory influence.² Here, we found increased activation in the PAG during stimulus *delivery* when DLPFC engagement had been high during stimulus *anticipation* (Fig. 4). DLPFC and PAG are key nodes of the descending pain control system that implements opioid-mediated expectancy-related pain modulation.^{2,35,59} Engagement of this system is commonly described as eliciting a direct influence on dorsal horn nociceptive processing. However, our results suggest a link to biased decision-making (change in starting point) - a process that is believed to be different from sensory processing (change in drift rate). While a shift in starting point is implemented when relevant information becomes available (i.e., prior to stimulus delivery), drift rate is tied to stimulus processing itself. Because the drift-diffusion model used here does not allow for single-trial estimates, our data is not suited to probe the functional relevance of the observed DLPFC and PAG involvement in more detail. One could, however, speculate that prior information leads to a shift in starting point at the time the information becomes available (as reflected in DLPFC

engagement) but it is implemented through altered sensory processing (e.g., as implemented via antinociceptive processing in the PAG) during stimulus application. Of note, significantly increased PAG activity during stimulus processing was only found when the expected high-intensity stimulation was applied but not when the high-intensity cue was followed by low-intensity stimulation or when participants had been cued towards low pain. In principle, PAG engagement could depend on expected outcome, on stimulation intensity – or a combination of the two factors (e.g., it mainly occurs when the stimulation is expected *and* of a high intensity). Our findings support the latter and suggest that PAG involvement during stimulus delivery might be most prominent in scenarios in which antinociceptive counter-regulation – one of the key PAG functions³¹ – is required due to high intensity stimulation and facilitated through correct prior knowledge.

A second key finding of our study is the link between an increase in drift rate, engagement of the amygdala (Fig. 5) and an increase in its functional connectivity with the PAG (Fig. 6) during unexpected high-intensity stimulation. The unexpected delivery of a high-intensity stimulus can be regarded as the ‘worst case scenario’ in our paradigm and should evoke an aversive prediction error (PE). A multitude of studies have implicated the amygdala in aversive PE processing, showing that amygdala neurons respond preferentially to unexpected aversive stimuli.^{6,32,34,38,47} Our observation extends these findings by demonstrating a link between PE-related amygdala activation and a change in drift rate which is often interpreted as accelerated sensory processing during evidence accumulation. ‘Fast tracking’ of incoming information seems adaptive when strong aversive input occurs unexpectedly, as only immediate changes in behaviour (e.g., escape or attack) may

prevent further harm. Based on findings showing that impaired amygdala functioning abolishes heightened responses to fear-related stimuli in primary sensory brain regions^{28,55,64}, the amygdala has been proposed to prioritize processing of emotionally relevant stimuli through gain control in these areas.^{11,51} Our data seem not to support this notion. Although activation in the left amygdala was positively correlated with change in drift rate during unexpected high-intensity stimulation (Fig. 5), we found no evidence for altered processing in brain regions implicated in nociceptive processing (including thalamus, posterior insula, primary or secondary somatosensory cortex) or change in functional connectivity between the amygdala and these brain regions.

However, recent investigations into the neural network underlying fear learning and its influence on sensory processing have focused on amygdala interactions with another structure – the PAG. Unexpected aversive stimuli generate PE responses in the PAG that serve as a teaching signal to drive learning and fear-related plasticity.^{32,39} Notably, PE signaling in the PAG has recently also been demonstrated in the context of pain in humans.⁵⁶ Here, we found an increase in amygdala - PAG connectivity that scaled with the increase in drift rate during unexpected high-intensity stimulation (Fig. 6).

The lack of modulation in sensory brain regions and the involvement of amygdala and PAG which are both key regions of affective processing cast doubt on the exclusive interpretation of an increase in drift rate as amplified processing in sensory brain regions. As pointed out previously⁴², brain activity related to differences in drift rate could also reflect collinear cognitive processes such as attention, motivation or preparation of motor responses. The involvement of specific brain regions would thereby depend on the type of information accumulated. Amygdala engagement is in

line with growing evidence showing that expectancy manipulations of pain are not necessarily found in brain regions involved in sensory processing⁷³ but might be reflected in regions associated with affective processing.² Increased drift rates might therefore reflect the fast propagation of information within a system that ensures swift responses to impending threat, potentially including counter-regulatory processes. With fast amygdala responses to threat⁴⁰ (which arise prior to conscious perception⁴) and connections with key regions of behavioural responses to threat, the amygdala is ideally suited to serve this function.

The findings of this study have to be seen in light of some limitations. First, given that the findings are based on a relatively small sample size, larger-scale follow-up investigations are needed for confirmation, particularly before conclusions can be drawn regarding clinical implications. Second, while we used stringent voxel-wise permutation testing with family-wise error correction for multiple comparisons, we did not correct for the number of ROIs included. Third, as we only compared an 80% and a 20% probability (in addition to the 50% condition that served as a control), it remains unclear to what extent our findings generalize to other probability splits. Fourth, individuals can be more or less certain about their perceptual decision which is known to influence the effect of prior information on perception⁷⁰. Future studies should therefore ideally include trial-by-trial measures of uncertainty to inform data analysis.

Conclusions

Our findings emphasize the relevance of affect-related considerations and accompanying cortico-brainstem interactions when investigating the neural basis of

perceptual decision-making and underscore the growing call for the use of computational models in this endeavor.⁵⁴ Additional studies are needed to further explore the role of stimulus valence including its link to motivational aspects and learning which embed perceptual decisions into the context of the individual's priorities. Such integration, particularly when combined with insights into interindividual differences including personality traits, promises a novel and more comprehensive view on pain-related perceptual decision-making.

References

1. Atlas LY, Bolger N, Lindquist MA, Wager TD: Brain mediators of predictive cue effects on perceived pain. *J Neurosci* 30:12964–12977, 2010.
2. Atlas LY, Wager TD: A meta-analysis of brain mechanisms of placebo analgesia: consistent findings and unanswered questions. In: Benedetti F, Enck P, Frisaldi E, Schedlowski M, editors. Berlin, Heidelberg: Springer Berlin Heidelberg; page 37–69, 2014.
3. Atlas LY, Whittington RA, Lindquist MA, Wielgosz J, Sonty N, Wager TD: Dissociable influences of opiates and expectations on pain. *J Neurosci* 32:8053–8064, 2012.
4. Bastuji H, Frot M, Perchet C, Magnin M, Garcia-Larrea L: Pain networks from the inside: spatiotemporal analysis of brain responses leading from nociception to conscious perception. *Hum Brain Mapp* 37:4301–4315, 2016.
5. Behrens TEJ, Johansen-Berg H, Woolrich MW, Smith SM, Wheeler-Kingshott CAM, Boulby PA, Barker GJ, Sillery EL, Sheehan K, Ciccarelli O: Non-invasive mapping of connections between human thalamus and cortex using diffusion imaging. *Nat Neurosci* 6:750, 2003.
6. Belova MA, Paton JJ, Morrison SE, Salzman CD: Expectation modulates neural responses to pleasant and aversive stimuli in primate amygdala. *Neuron* 55:970–984, 2007.
7. Bingel U, Lorenz J, Schoell E, Weiller C, Buchel C: Mechanisms of placebo analgesia: rACC recruitment of a subcortical antinociceptive network. *Pain* 120:8–15, 2006.

8. Bingel U, Wanigasekera V, Wiech K, Ni Mhuircheartaigh R, Lee MC, Ploner M, Tracey I: The effect of treatment expectation on drug efficacy: imaging the analgesic benefit of the opioid remifentanyl. *Sci Transl Med* 3:70ra14, 2011.
9. Bonaiuto JJ, Berker A de, Bestmann S: Response repetition biases in human perceptual decisions are explained by activity decay in competitive attractor models. *eLife* 5:e20047, 2016.
10. Cardoso-Leite P, Waszak F, Lepsien J: Human perceptual decision making: Disentangling task onset and stimulus onset. *Hum Brain Mapp* 35:3170–3187, 2014.
11. Chen Y, Li H, Jin Z, Shou T, Yu H: Feedback of the amygdala globally modulates visual response of primary visual cortex in the cat. *NeuroImage* 84:775–785, 2014.
12. Deichmann R, Gottfried J, Hutton C, Turner R: Optimized EPI for fMRI studies of the orbitofrontal cortex. *NeuroImage* 19:430–441, 2003.
13. Desikan RS, Ségonne F, Fischl B, Quinn BT, Dickerson BC, Blacker D, Buckner RL, Dale AM, Maguire RP, Hyman BT, Albert MS, Killiany RJ: An automated labeling system for subdividing the human cerebral cortex on MRI scans into gyral based regions of interest. *NeuroImage* 31:968–980, 2006.
14. Diedrichsen J, Shadmehr R: Detecting and adjusting for artifacts in fMRI time series data. *NeuroImage* 27:624–634, 2005.

15. Domenech P, Dreher J-C: Decision threshold modulation in the human brain. *J Neurosci Off J Soc Neurosci* 30:14305–14317, 2010.
16. Eickhoff SB: The human parietal operculum. I. Cytoarchitectonic mapping of subdivisions. *Cereb Cortex* 16:254–267, 2005.
17. Eickhoff SB: The human parietal operculum. II. Stereotaxic maps and correlation with functional imaging results. *Cereb Cortex* 16:268–279, 2005.
18. Eickhoff SB, Stephan KE, Mohlberg H, Grefkes C, Fink GR, Amunts K, Zilles K: A new SPM toolbox for combining probabilistic cytoarchitectonic maps and functional imaging data. *NeuroImage* 25:1325–1335, 2005.
19. Eippert F, Bingel U, Schoell ED, Yacubian J, Klinger R, Lorenz J, Büchel C: Activation of the opioidergic descending pain control system underlies placebo analgesia. *Neuron* 63:533–543, 2009.
20. Ezra M, Faull OK, Jbabdi S, Pattinson KT: Connectivity-based segmentation of the periaqueductal gray matter in human with brainstem optimized diffusion MRI: segmentation of the PAG with Diffusion MRI. *Hum Brain Mapp* 36:3459–3471, 2015.
21. Fast CD, McGann JP: Amygdalar gating of early sensory processing through interactions with locus coeruleus. *J Neurosci* 37:3085–3101, 2017.
22. Friston K, Buechel C, Fink G, Morris J, Rolls E, Dolan R: Psychophysiological and modulatory interactions in neuroimaging. *Neuroimage* 6:218–229, 1997.

23. Froehlich E, Liebig J, Ziegler JC, Braun M, Lindenberger U, Heekeren HR, Jacobs AM: Drifting through basic subprocesses of reading: A hierarchical diffusion model analysis of age effects on visual word recognition. *Front Psychol* 7:1863, 2016.
24. Fruhstorfer H, Lindblom U, Schmid WC: Method for quantitative estimation of thermal thresholds in patients. *J Neurol Neurosurg Psychiatry* 39:1071, 1976.
25. Geyer S, Schleicher A, Zilles K: Areas 3a, 3b, and 1 of human primary somatosensory cortex. *Neuroimage* 10:63–83, 1999.
26. Geyer S, Schormann T, Mohlberg H, Zilles K: Areas 3a, 3b, and 1 of human primary somatosensory cortex 2. Spatial normalization to standard anatomical space. *NeuroImage* 11:684–696, 2000.
27. Grefkes C, Geyer S, Schormann T, Roland P, Zilles K: Human somatosensory area 2: observer-independent cytoarchitectonic mapping, interindividual variability, and population map. *NeuroImage* 14:617–631, 2001.
28. Hadj-Bouziane F, Liu N, Bell AH, Gothard KM, Luh W-M, Tootell RBH, Murray EA, Ungerleider LG: Amygdala lesions disrupt modulation of functional MRI activity evoked by facial expression in the monkey inferior temporal cortex. *Proc Natl Acad Sci* 109:E3640–3648, 2012.
29. Heekeren HR, Marrett S, Bandettini PA, Ungerleider LG: A general mechanism for perceptual decision-making in the human brain. *Nature* 431:859–862, 2004.

30. Heekeren HR, Marrett S, Ungerleider LG: The neural systems that mediate human perceptual decision making. *Nat Rev Neurosci* 9:467–479, 2008.
31. Heinricher MM, Fields HL: Central nervous system mechanisms of pain modulation. *Wall Melzack's Textb Pain* 6th ed. London: Elsevier; page 129–142, 2013.
32. Johansen JP, Tarpley JW, LeDoux JE, Blair HT: Neural substrates for expectation-modulated fear learning in the amygdala and periaqueductal gray. *Nat Neurosci* 13:979–986, 2010.
33. Keltner J, Furst A, Fan C, Redfern R, Inglis B, Fields H: Isolating the modulatory effect of expectation on pain transmission: a functional magnetic resonance imaging study. *J Neurosci* 26:4437–4443, 2006.
34. Klavir O, Genuit-Gabai R, Paz R: Functional connectivity between amygdala and cingulate cortex for adaptive aversive learning. *Neuron* 80:1290–1300, 2013.
35. Krummenacher P, Candia V, Folkers G, Schedlowski M, Schonbachler G: Prefrontal cortex modulates placebo analgesia. *Pain* 148:368–374, 2010.
36. Kurth F, Eickhoff SB, Schleicher A, Hoemke L, Zilles K, Amunts K: Cytoarchitecture and probabilistic maps of the human posterior insular cortex. *Cereb Cortex* 20:1448–1461, 2010.
37. Lorenz J, Minoshima S, Casey KL: Keeping pain out of mind: the role of the dorsolateral prefrontal cortex in pain modulation. *Brain J Neurol* 126:1079–1091, 2003.

38. McHugh SB, Barkus C, Huber A, Capitaó L, Lima J, Lowry JP, Bannerman DM: Aversive prediction error signals in the amygdala. *J Neurosci* 34:9024–9033, 2014.
39. McNally GP, Johansen JP, Blair HT: Placing prediction into the fear circuit. *Trends Neurosci* 34:283–292, 2011.
40. Méndez-Bértolo C, Moratti S, Toledano R, Lopez-Sosa F, Martínez-Alvarez R, Mah YH, Vuilleumier P, Gil-Nagel A, Strange BA: A fast pathway for fear in human amygdala. *Nat Neurosci* 19:1041–1049, 2016.
41. Moeller S, Yacoub E, Olman CA, Auerbach E, Strupp J, Harel N, Uğurbil K: Multiband multislice GE-EPI at 7 tesla, with 16-fold acceleration using partial parallel imaging with application to high spatial and temporal whole-brain fMRI. *Magn Reson Med* 63:1144–1153, 2010.
42. Mulder MJ, van Maanen L, Forstmann BU: Perceptual decision neurosciences – A model-based review. *Neuroscience* 277:872–884, 2014.
43. Mulder MJ, Wagenmakers EJ, Ratcliff R, Boekel W, Forstmann BU: Bias in the brain: A diffusion model analysis of prior probability and potential payoff. *J Neurosci* 32:2335–2343, 2012.
44. Nagano-Saito A, Cisek P, Perna AS, Shirdel FZ, Benkelfat C, Leyton M, Dagher A: From anticipation to action, the role of dopamine in perceptual decision making: an fMRI-tyrosine depletion study. *J Neurophysiol* 108:501–512, 2012.

45. Neubert F-X, Mars RB, Sallet J, Rushworth MFS: Connectivity reveals relationship of brain areas for reward-guided learning and decision making in human and monkey frontal cortex. *Proc Natl Acad Sci* 112:E2695–2704, 2015.
46. Ozawa T, Johansen JP: Learning rules for aversive associative memory formation. *Curr Opin Neurobiol* 49:148–157, 2018.
47. Ozawa T, Ycu EA, Kumar A, Yeh L-F, Ahmed T, Koivumaa J, Johansen JP: A feedback neural circuit for calibrating aversive memory strength. *Nat Neurosci* 20:90–97, 2016.
48. Philiastides MG, Aukstulewicz R, Heekeren HR, Blankenburg F: Causal role of dorsolateral prefrontal cortex in human perceptual decision making. *Curr Biol* 21:980–983, 2011.
49. Ploghaus A, Narain C, Beckmann CF, Clare S, Bantick S, Wise R, Matthews PM, Rawlins JN, Tracey I: Exacerbation of pain by anxiety is associated with activity in a hippocampal network. *J Neurosci* 21:9896–9903, 2001.
50. Poldrack RA, Baker CI, Durnez J, Gorgolewski KJ, Matthews PM, Munafò MR, Nichols TE, Poline J-B, Vul E, Yarkoni T: Scanning the horizon: towards transparent and reproducible neuroimaging research. *Nat Rev Neurosci* 18:115–126, 2017.
51. Pourtois G, Schettino A, Vuilleumier P: Brain mechanisms for emotional influences on perception and attention: What is magic and what is not. *Biol Psychol* 92:492–512, 2013.

52. Pruim RHR, Mennes M, van Rooij D, Llera A, Buitelaar JK, Beckmann CF: ICA-AROMA: A robust ICA-based strategy for removing motion artifacts from fMRI data. *NeuroImage* 112:267–277, 2015.
53. Ratcliff R: A theory of memory retrieval. *Psychol Rev* 85:59–108, 1978.
54. Roberts ID, Hutcherson CA: Affect and decision making: insights and predictions from computational models. *Trends Cogn Sci* 23:602–614, 2019.
55. Rotshtein P, Richardson MP, Winston JS, Kiebel SJ, Vuilleumier P, Eimer M, Driver J, Dolan RJ: Amygdala damage affects event-related potentials for fearful faces at specific time windows. *Hum Brain Mapp* 31:1089–1105, 2009.
56. Roy M, Shohamy D, Daw N, Jepma M, Wimmer GE, Wager TD: Representation of aversive prediction errors in the human periaqueductal gray. *Nat Neurosci* 17:1607–1612, 2014.
57. Sallet J, Mars RB, Noonan MP, Neubert F-X, Jbabdi S, O'Reilly JX, Filippini N, Thomas AG, Rushworth MF: The Organization of Dorsal Frontal Cortex in Humans and Macaques. *J Neurosci* 33:12255–12274, 2013.
58. Seminowicz DA, Moayedil M: The dorsolateral prefrontal cortex in acute and chronic pain. *J Pain* 18:1027–1035, 2017.
59. Stein N, Sprenger C, Scholz J, Wiech K, Bingel U: White matter integrity of the descending pain modulatory system is associated with interindividual differences in placebo analgesia. *Pain* 153:2210–2217, 2012.

60. Steinweg B, Mast FW: Semantic incongruity influences response caution in audio-visual integration. *Exp Brain Res* 235:349–363, 2017.
61. Tovote P, Esposito MS, Botta P, Chaudun F, Fadok JP, Markovic M, Wolff SBE, Ramakrishnan C, Fenno L, Deisseroth K, Herry C, Arber S, Lüthi A: Midbrain circuits for defensive behaviour. *Nature* 534:206–212, 2016.
62. Tracey I: Getting the pain you expect: mechanisms of placebo, nocebo and reappraisal effects in humans. *Nat Med* 16:1277–1283, 2010.
63. Vandekerckhove J, Tuerlinckx F, Lee MD: Hierarchical diffusion models for two-choice response times. *Psychol Methods* 16:44–62, 2011.
64. Vuilleumier P, Richardson MP, Armony JL, Driver J, Dolan RJ: Distant influences of amygdala lesion on visual cortical activation during emotional face processing. *Nat Neurosci* 7:1271–1278, 2004.
65. Wager TD, Rilling JK, Smith EE, Sokolik A, Casey KL, Davidson RJ, Kosslyn SM, Rose RM, Cohen JD: Placebo-induced changes in FMRI in the anticipation and experience of pain. *Science* 303:1162–1167, 2004.
66. White CN, Mumford JA, Poldrack RA: Perceptual criteria in the human brain. *J Neurosci* 32:16716–16724, 2012.
67. Wiech K, Vandekerckhove J, Zaman J, Tuerlinckx F, Vlaeyen JWS, Tracey I: Influence of prior information on pain involves biased perceptual decision-making. *Curr Biol* 24:R679–681, 2014.

68. Winkler AM, Webster MA, Brooks JC, Tracey I, Smith SM, Nichols TE: Non-parametric combination and related permutation tests for neuroimaging: NPC and related permutation tests for neuroimaging. *Hum Brain Mapp* 37:1486–1511, 2016.
69. Xu J, Moeller S, Auerbach EJ, Strupp J, Smith SM, Feinberg DA, Yacoub E, Uğurbil K: Evaluation of slice accelerations using multiband echo planar imaging at 3T. *NeuroImage* 83:991–1001, 2013.
70. Yoshida W, Seymour B, Koltzenburg M, Dolan RJ: Uncertainty increases pain: evidence for a novel mechanism of pain modulation involving the periaqueductal gray. *J Neurosci* 33:5638–5646, 2013.
71. Zaman J, Madden VJ, Iven J, Wiech K, Weltens N, Ly HG, Vlaeyen JWS, Van Oudenhove L, Van Diest I: Biased intensity judgements of visceral sensations after learning to fear visceral stimuli: a drift diffusion approach. *J Pain* 18:1197–1208, 2017.
72. Zaman J, Wiech K, Claes N, Van Oudenhove L, Van Diest I, Vlaeyen JWS: The influence of pain-related expectations on intensity perception of non-painful somatosensory stimuli: *Psychosom Med* 80:836–844, 2018.
73. Zunhammer M, Bingel U, Wager TD, for the Placebo Imaging Consortium: Placebo effects on the Neurologic Pain Signature: a meta-analysis of individual participant functional magnetic resonance imaging data. *JAMA Neurol* 75:1321–1330, 2018.

Figures

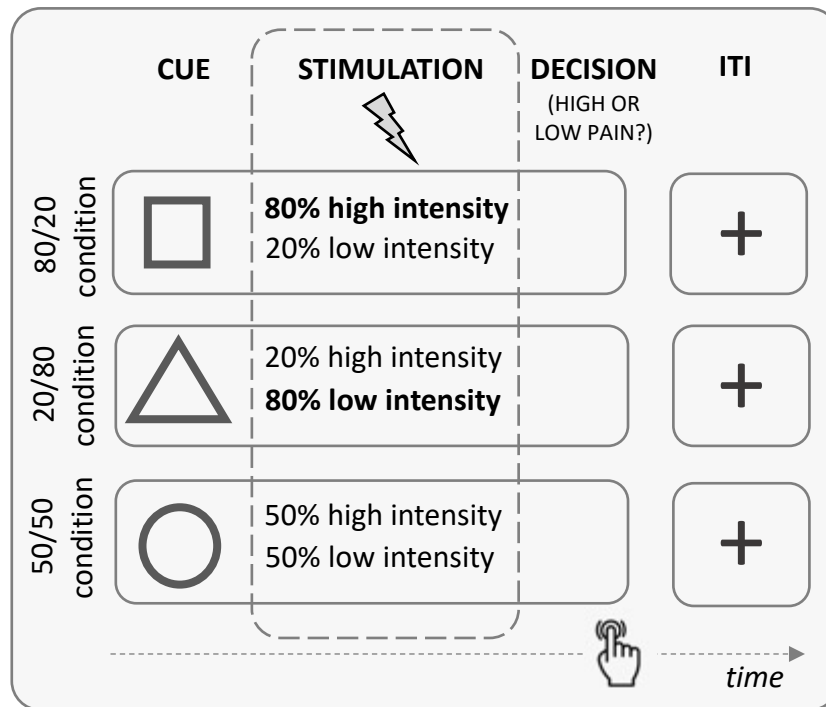


Figure 1. Overview of the experimental paradigm and trial structure. On each trial, participants were presented with one of three visual cues ('cue' period). One of the cues indicated an 80% probability for high-intensity stimulation and a 20% probability for low intensity stimulation ('80/20' condition). Another cue indicated a 20% probability for high-intensity stimulation and an 80% probability for low intensity stimulation ('20/80' condition). A third cue signalled a 50% probability for high-intensity stimulation and a 50% probability for low intensity stimulation ('50/50' condition). Upon stimulus delivery ('stimulation' period) participants indicated as quickly and accurately as possible whether they had received low-intensity or high-intensity stimulation by pressing one of two buttons with their right hand ('decision' period). Each trial was completed by the presentation of a fixation cross (inter-trial interval, 'ITI').

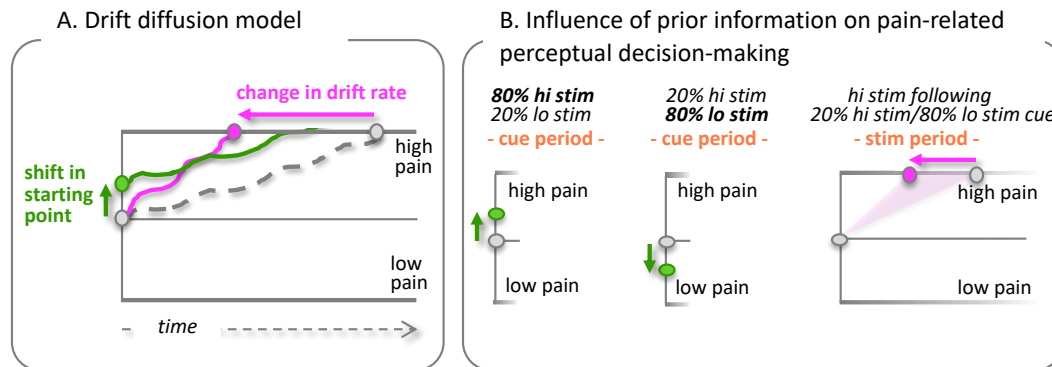


Figure 2. Overview of the Drift Diffusion Model (DDM) and previous behavioural findings. (A) The Drift Diffusion Model conceptualizes binary perceptual decisions as an inferential process in which sensory evidence is accumulated over time and the decision is made as soon as the upper or lower boundary is reached. The process is characterized by different parameters including the mean starting point (β) and the speed at which evidence is accumulated (i.e., the drift rate, δ). Prior information can bias the perceptual process through any of the parameters (unbiased process shown as dashed line). The graph separately depicts a shift in starting point (indicating a bias in decision-making; shown in green) and an increase in drift rate (indicating faster sensory processing; shown in magenta). **(B)** We previously demonstrated that a visual cue signaling an 80% probability to receive a high-intensity stimulation and 20% probability for low-intensity stimulation leads to a shift in starting point towards the high pain boundary relative to a 50/50 condition⁶⁷ (left panel). Similarly, a cue signaling a 20% probability for high-intensity and 80% for low intensity shifts the starting point towards low pain (mid panel). If a high-intensity stimulus is delivered following the presentation of cue signaling a 20% probability for high-intensity and 80% probability for low-intensity stimulation, an increase in drift rate is found (right panel). hi stim= high-intensity stimulation; lo stim= low-intensity stimulation; stim period= stimulation period.

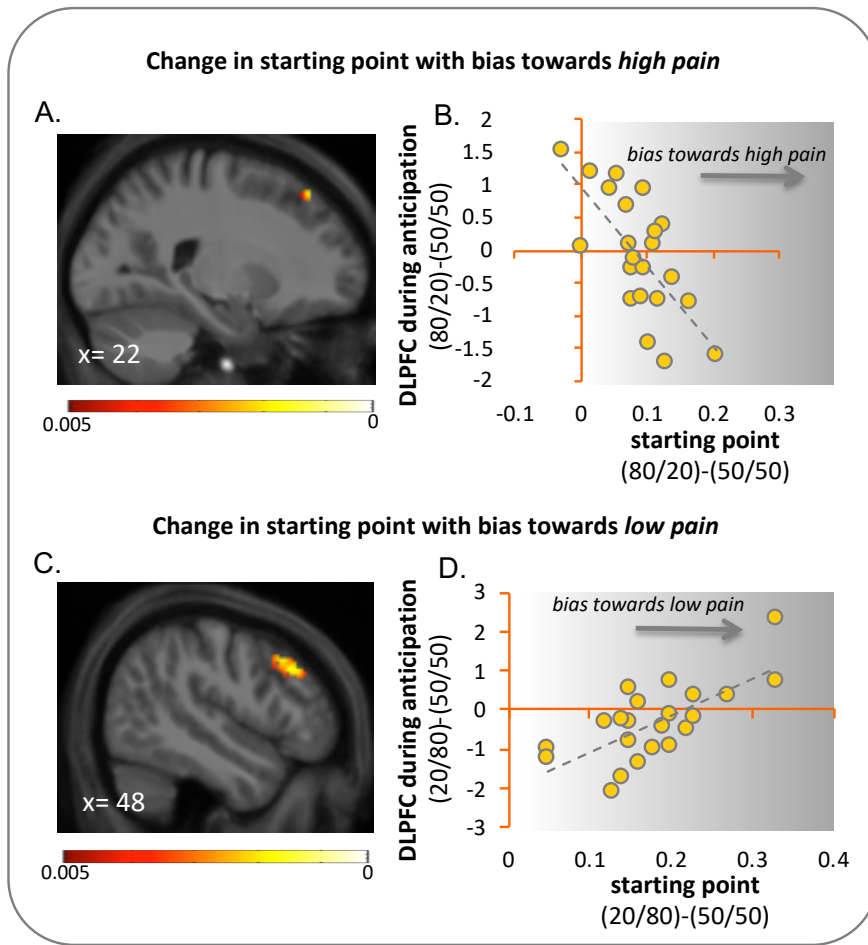


Figure 3. DLPFC activation related to a shift in starting point. **(A)** DLPFC activity exhibiting a *negative* correlation with change in starting point when high-intensity stimulation was the more likely outcome relative to the condition when both stimulation intensities were equally likely ('80/20' minus '50/50'; thresholded at $p < 0.005$ uncorrected for display purpose; overlaid on group mean T1 image masked by DLPFC region-of-interest). **(B)** Illustrative scatter plot showing the relationship between change in starting point ('80/20' minus '50/50') and activation in the peak voxel of the DLPFC ('80/20' minus '50/50'). **(C)** DLPFC activation exhibiting a *positive* correlation with change in starting point towards the low pain boundary when low-intensity stimulation was the most likely outcome relative to the condition when both stimulation intensities were equally likely ('20/80' minus '50/50'; thresholded at $p < 0.005$ uncorrected for display purpose; overlaid on group mean T1 image masked by DLPFC region-of-interest). **(D)** Illustrative scatter plot showing the relationship between change in starting point ('20/80' minus '50/50') and activation in the peak voxel of the DLPFC ('20/80' minus '50/50'). Note that the x-axis shows the absolute difference in starting point between both conditions ($| \text{'20/80' minus '50/50'} |$).

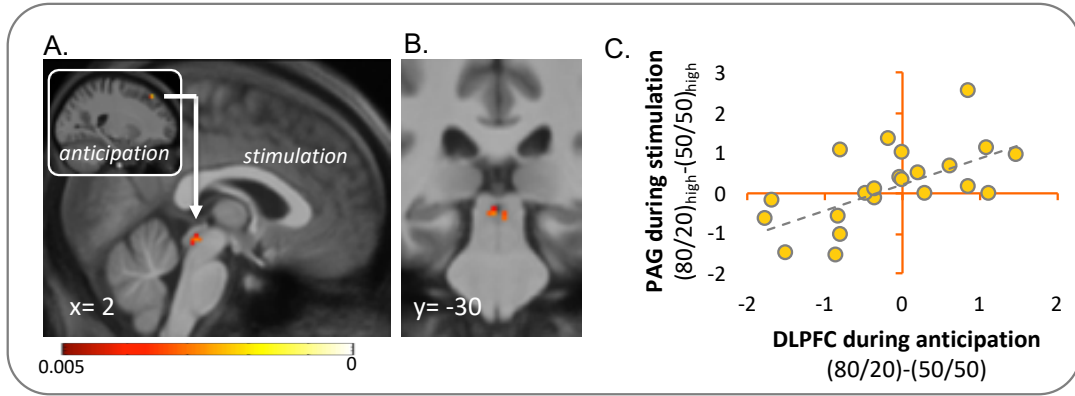


Figure 4. DLPFC-related PAG responses during the stimulation period. (A) Differential DLPFC activity (shown in inset) during the *anticipation* of high-intensity stimulation (relative to the '50/50' condition) was used as a covariate in the analysis of activity during high-intensity *stimulation* following the '80/20' cue (relative to the '50/50' cue). DLPFC activity was extracted from the peak voxel identified in Analysis 1. **(A)** Sagittal view and **(B)** coronal view of the activation cluster in the PAG during delivery of the expected high-intensity stimuli (thresholded at $p < 0.005$ uncorrected for display purpose; overlaid on group mean T1 image masked by PAG region-of-interest). **(C)** The illustrative scatter plot shows the positive correlation between differential ('80/20' minus '50/50') anticipatory DLPFC activity and differential ('80/20' minus '50/50') PAG activity during delivery of high-intensity stimulation across the sample.

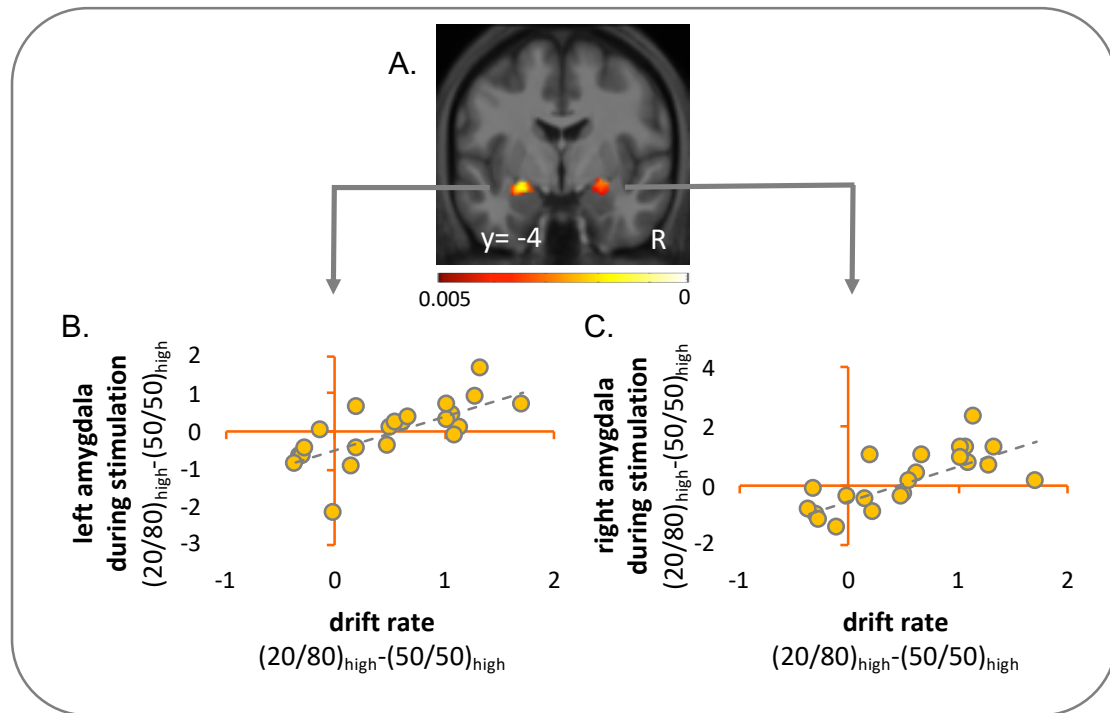


Figure 5. Drift-rate related activity in the amygdala during unexpected delivery of high-intensity stimuli. (A) Activity in left and right amygdala during the delivery of high-intensity stimulation following the presentation of the safe cue ('20/80_high') scaled with an increase in drift rate (both relative to the neutral '50/50' condition; thresholded at $p < 0.005$ uncorrected for display purpose; overlaid on group mean T1 image masked by amygdala region-of-interest). Illustrative scatter plots from the amygdala peak voxels show the correlation between the condition difference in drift rate and activation in the left **(B)** and right **(C)** amygdala across the sample.

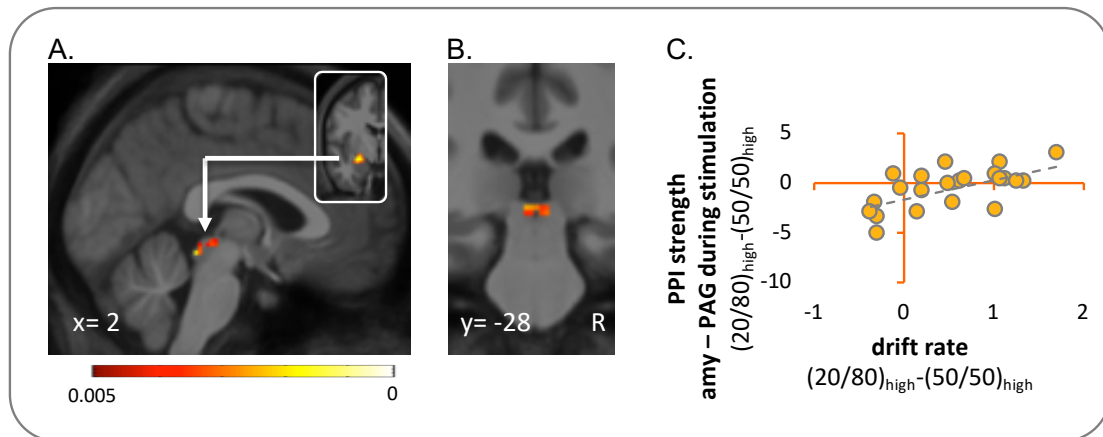


Figure 6. Drift-rate related functional connectivity between amygdala and PAG during unexpected delivery of high-intensity stimuli. (A) Sagittal and **(B)** coronal view of the PAG showing increased functional connectivity with the left amygdala (inset) during the unexpected delivery of high-intensity stimuli (relative to high intensity stimulation following the '50/50' cue; '20/80_high' minus '50/50_high') depending on drift rate ('20/80_high' minus '50/50_high'). Thresholded at $p < 0.005$ uncorrected for display purpose; overlaid on group mean T1 image masked by PAG region-of-interest. **(C)** Illustrative scatter plot from the PAG peak voxel shows the correlation between the condition difference in drift rate and PPI strength between the left amygdala and PAG across the sample.